Cumhuriyet Sci. J., 46(4) (2025) 780-790
DOI: https://doi.org/10.17776/csj.1733240

Cumhuriyet Science Journal

| csj.cumhuriyet.edu.tr | Founded: 2002 ISSN: 2587-2680 e-ISSN: 2587-246X Publisher: Sivas Cumhuriyet University

Design, Synthesis, and Thermal Characterization of N,N'-Dibutyl-1,6-Hexanediammonium Based Protic Ionic Liquids for Phase Change Energy Storage Applications

Derya Kahraman Döğüşcü [1,a,*], Hüseyin Akbaş [1,b]

[1]*Tokat Gaziosmanpaşa University, Department of Chemistry 60250, Tokat, Türkiye*

**Corresponding author*

Research Article

History
Received: 02/07/2025
Accepted: 15/10/2025

ABSTRACT

Protic ionic liquids (PILs) based on *N,N'*-Dibutyl-1,6-hexanediammonium were successfully synthesized using lauric, palmitic, and myristic acids as anionic counterparts for thermal energy storage (TES) materials. The structural characteristics of the resulting PILs were characterized using FT-IR, ^{1}H, and ^{13}C NMR spectroscopy, which confirmed effective proton transfer and the formation of ionic bonds between the cationic and anionic species. Thermal properties, including thermal stability were examined using differential scanning calorimetry (DSC) and thermogravimetric analysis (TGA). The values for the latent heat of fusion were recorded as 69.73, 88.73, and 98.95 kJ/mol for PIL1, PIL2, and PIL3, respectively. Moreover, the synthesized PILs exhibit thermal stability up to around 463.15 K. The synthesized PILs showed strong thermal stability and appropriate phase change temperatures, indicating their suitability as PCMs for TES systems. This study provides insights into the design and development of novel PILs tailored for efficient and sustainable energy storage applications.

Key words: Protic ionic liquid, Phase change material, Fatty acid

[a] *derya.kahraman@gop.edu.tr* *https://orcid.org/0000-0002-6181-5778* [b] *huseyin.akbas@gop.edu.tr* *https://orcid.org/0000-0002-3013-9033*

Introduction

The rise in global energy consumption is primarily driven by factors such as urbanization, industrial growth, and population increase [1,2]. In response to pressing global challenges like climate change and the growing energy demand, the need for long-term, environmentally sustainable energy solutions is becoming increasingly urgent. Currently, over 18% of the world's energy consumption is sourced from renewables [3]. Renewable energy is favored over non-renewable resources due to its sustainable availability, accessibility, and positive environmental impact. However, the intermittent nature of renewable sources like solar and wind energy creates challenges for their integration, as their variable supply complicates the assurance of a stable energy output [4]. Thermal energy storage (TES) is a key technology advancing the goal of a carbon-free future. Achieving a low-carbon energy system is possible by combining renewable energy sources with various TES systems that can reach round-trip efficiencies above 96% [5,6]. TES significantly contributes to improving sustainability and energy efficiency by reducing dependence on fossil fuels. It enables the storage of excess energy when generation surpasses demand and helps bridge the gap during peak consumption periods, thus addressing the variability inherent to renewable energy [7]

TES systems have the capacity to either absorb or release energy while maintaining a constant temperature, achieving reduced volume change and lower vapor pressure through the utilization of phase change materials (PCMs), which function as units for latent heat storage [8,9]. PCMs represent a significant advancement in the storage of substantial quantities of latent thermal energy, effectively sustaining a nearly constant temperature throughout phase transitions, which may include solid-solid, solid-liquid, liquid-gas or solid-gas transformations [10]. The efficacy of phase change energy storage is contingent upon the latent heat of the material, the temperature range, and various system characteristics. In this context, liquid to gas transformation typically sustains the highest energy level. It is essential to acknowledge that these systems typically necessitate significant temperature differentials and high pressure, as overall efficiency is contingent upon the materials employed, the design, and the specific application requirements. Solid-liquid phase change is an effective process that conserves heat during the phase transition and generally facilitates lower temperature differentials. The latent heat of fusion is generally lower; however, the system's simplified design renders it appropriate for low-temperature applications [11–14].

PCMs are classified into three main categories: organic, inorganic, and eutectic [15]. Organic PCMs are further divided into paraffins and non-paraffins. The non-paraffin group includes a variety of organic compounds such as fatty acids, esters, alcohols, and glycols [16].

Inorganic PCMs consist of salt hydrates, molten salts, metals, or metal alloys, though metals and alloys typically have melting points too high for passive building applications [12,17–19]. A eutectic PCM is defined as a mixture of two or more components that melt and solidify at the lowest possible melting point for the mixture, undergoing congruent melting and solidification to form a mixture of the original crystals during phase change. Eutectic PCMs can be grouped into three types: inorganic–inorganic, organic–organic, and organic–inorganic [20,21]. The choice between inorganic and organic PCMs in thermal energy storage systems depends on their specific benefits and drawbacks. Inorganic PCMs are advantageous due to their high latent heat capacity, relatively greater thermal conductivity, non-toxicity, non-flammability, and generally lower cost compared to organic PCMs [22,23]. They show great promise for use in building construction [24–26], concentrated solar power plants [27,28], and thermal management of lithium-ion batteries [29–32], among other applications. However, latent heat storage materials face challenges related to the specific PCM used, including issues like phase segregation, low thermal conductivity, supercooling, leakage, flammability, and thermal instability. Problems such as supercooling and phase segregation can be mitigated by adding thickening or nucleating agents, arranging thin layers horizontally, or employing mechanical stirring techniques [33–36].

Ionic liquids (ILs) are a class of molten salts composed of organic cations paired with inorganic or organic anions, typically exhibiting melting points below 100 °C. ILs are categorized into two main groups based on their structural characteristics: protic ILs (PILs) and aprotic ILs (AILs). PILs are formed through a Brønsted acid-base reaction involving the transfer of a proton from a Brønsted acid to a Brønsted base, leading to the formation of ionic species - cations and anions - that interact via electrostatic forces. This synthetic approach is considered one of the simplest and most cost-effective methods for producing PILs, owing to its single-step nature, solvent-free conditions, and high efficiency. PILs are recognized as functional materials used in a wide range of applications and are being investigated as PCMs for TES. The utilization of specific types of ILs in thermal storage systems represents an innovative approach. Within this context, critical properties such as thermal stability are typically examined comprehensively using thermogravimetric analysis techniques. Research on the use of PILs as PCMs is relatively scarce in existing literature. The following is a summary of studies on this subject .

Mokhtarpour et al. characterized bis(2-hydroxyethyl)ammonium, 2-hydroxyethylammonium, and tris(2-hydroxyethyl)ammonium palmitate ILs as PCM functioning within the temperature spectrum of 30-100 °C. The synthesized ILs exhibited an energy storage capacity ranging from 123.2 to 158.9 J/g [37]. Mokhtarpour et al. carried out a synthesis of three distinct ionic liquids in a subsequent study published in 2024. The examination of the structural and thermal features of the materials, capable of storing an impressive 171.12 J/g of energy while maintaining 99.5% thermal stability, was conducted with meticulous attention to detail [38]. In a subsequent investigation released by the group within the same year, tris(2-hydroxyethyl)ammonium,bis(2hydroxyethyl)ammonium, and 2-hydroxyethylammonium laurate ionic liquids were assessed as phase change materials [39]. A recent study from 2023 examined the synthesis and thermophysical properties of dialkylammonium-based ILs utilized as solid-solid PCMs. The synthesized ionic liquids demonstrated promise for application as PCMs in TES systems at temperatures beneath 45 °C [40]. Faraji et al. synthesized compounds including lactate anions which serve as PCMs in the context of PILs. The synthesized ILs have been asserted to possess high thermal stability along with appropriate physical and chemical properties for TES [41]. PIL/PCM composites were synthesized utilizing tris(2-hydroxyethylammonium) ionic liquid in conjunction with lauric, palmitic, and stearic acids, serving as energy storage materials [41]. The research published in 2025 examined the thermal properties of PILs synthesized using hexanoate, acetate, and glycolate anions alongside diethanolammonium and monoethanolammonium cations [42].

In light of the advantages of PILs outlined above, this study aims to comprehensively investigate the potential of PILs as TES materials. The synthesis and structural characterization of PILs were carried out, and their thermal energy storage capacity and thermal stability were thoroughly examined using DSC and TGA analysis. Based on the obtained data, the latent heat storage capacity and thermal behavior of PIL-based PCMs were evaluated, demonstrating their suitability for sustainable and high-efficiency energy storage applications. This approach is intended to make a significant contribution to the development of next-generation materials for future TES systems.

Experimental

Materials

PILs with three distinct chain lengths were synthesized without the necessity of additional precursor purification using fatty acids and *N,N'*-Dibutyl-1,6-hexanediamine (Sigma Aldrich, purity ≥99%). Merck Company supplied the lauric acid ($C_{12}H_{24}O_2$, purity ≥ 99%), myristic acid ($C_{14}H_{28}O_2$, purity ≥ 99%), and palmitic acid ($C_{16}H_{32}O_2$, purity ≥ 99%) utilized. Methanol (technical grade), selected as the solvent, was sourced from Tekkim Chemicals.

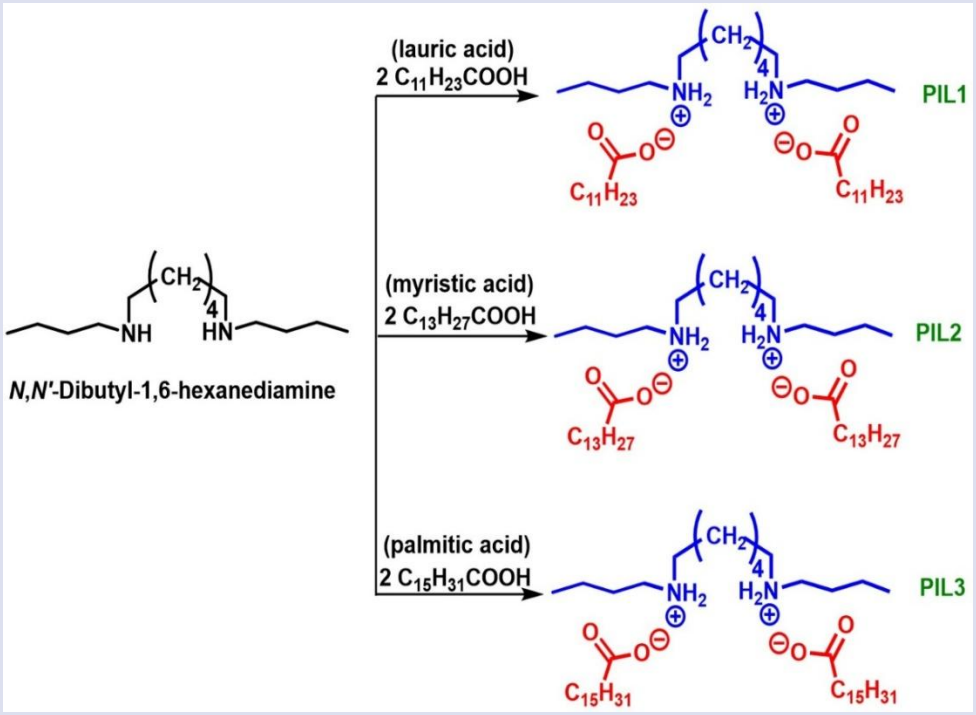

Figure 1. Schematic of the PILs

Synthesis

N,N'-Dibutyl-1,6-hexanediamine (1.00 g, 4.38 mmol) was dissolved in methanol, followed by the gradual addition of lauric acid (1.75 g, 8.76 mmol), myristic acid (2.00 g, 8.76 mmol), or palmitic acid (2.25 g, 8.76 mmol) in methanolic solution. The resulting mixture was stirred continuously in an ice bath for 24 hours. Subsequently, methanol was removed under reduced pressure. The obtained compounds were then dried in a vacuum oven at 60 °C for 48 hours to eliminate residual moisture formed during the reaction. Finally, the dried products were sealed with laboratory parafilm to prevent moisture contamination.

Method

The structural characterization of PILs was carried out using Fourier transform infrared spectroscopy (FT-IR) and nuclear magnetic resonance (^{1}H and ^{13}C NMR) techniques. FT-IR spectra were recorded on a JASCO FT-IR-4700 spectrometer (Japan) equipped with an attenuated total reflectance (ATR) accessory over a wavenumber range of 4000–400 cm^{-1}. The ^{1}H and ^{13}C NMR analyses were performed using a Bruker AVANCE III 400 MHz spectrometer with deuterated chloroform ($CDCl_3$) as the solvent. Chemical shifts were reported in parts per million (ppm) relative to tetramethylsilane (TMS) as an internal reference.

Thermal properties, including phase transition temperatures, melting and crystallization enthalpies, and total enthalpy, were determined by differential scanning calorimetry (DSC) using a Perkin Elmer Jade instrument calibrated with an indium standard. Measurements were conducted under a nitrogen atmosphere (flow rate of 60 mL/min) over a temperature range of 293.15 to 393.15 K (the temperature ranges below and above the melting and solidification temperatures of the synthesized PILs), employing a heating and cooling rate of 5 °C/min. Thermal stability, decomposition behavior, and onset temperatures of weight loss were evaluated via thermogravimetric analysis (TGA) using a Seteram TG-DTA/DSC analyzer. The instrument was calibrated with calcium oxalate and operated in a static air atmosphere over a temperature range of 308.15 to 773.15 K (thermal decomposition temperature range of the synthesized PILs) at a heating rate of 10 °C/min. The thermal reliability of the synthesized PCMs was assessed through 1000 thermal cycles using a BIOER TC-25/H thermal cycler. Each cycle consisted of heating and cooling between 293.15 and 393.15 K. Following thermal cycling, FT-IR and DSC analyses were repeated to verify both chemical and thermal stability.

Result And Discussion

Spectroscopic Characterization of the PILs

The structural properties of PILs formed by the protonation of *N,N'*-Dibutyl-1,6-hexanediamine with lauric, palmitic, and myristic acids were comprehensively evaluated using FT-IR and ^{1}H/^{13}C NMR spectroscopic techniquies. FT-IR spectroscopy is a valuable spectroscopic technique for elucidating the structural characteristics of salts. The FT-IR spectra of the PILs and lauric acid are presented in Figure 2. Additionally, the

characteristic absorption bands of the functional groups for all PILs are summarized in Table 1. The distinctive ammonium bands, corresponding to asymmetric and symmetric stretching vibrations, appear in the 3200-2500 cm^{-1} region. The asymmetric $\nu_{as}(NH_2^+)$ stretching vibration was observed as a medium-intensity band near 3025 cm^{-1}, whereas the symmetric $\nu_s(NH_2^+)$ stretching vibrations exhibited a broad band around 2372 cm^{-1}. The absorption band detected at approximately 1532 cm^{-1} is attributed to the N-H bending vibrations of the salts. The asymmetric and symmetric absorption bands of the carboxylate anion (COO^-) were identified at approximately 1629 $cm^{-1}$and 1397 cm^{-1}, respectively. The band observed near 1107 cm^{-1} corresponds to the stretching vibration of the C-N-C moiety in the cation. Moreover, the aliphatic C-H groups exhibited asymmetric and symmetric stretching vibrations at approximately 2919 cm^{-1} and 2850 cm^{-1}, respectively. When compared to the spectra of free acids, the FT-IR spectra of the salts displayed considerable variations. Notably, the characteristic C=O stretching band observed around 1696 cm^{-1} in free fatty acids was absent in the salt compounds. Furthermore, the presence of the $-NH_2^+$ and $-COO^-$ absorption bands in the salts provides definitive evidence of salt formation.

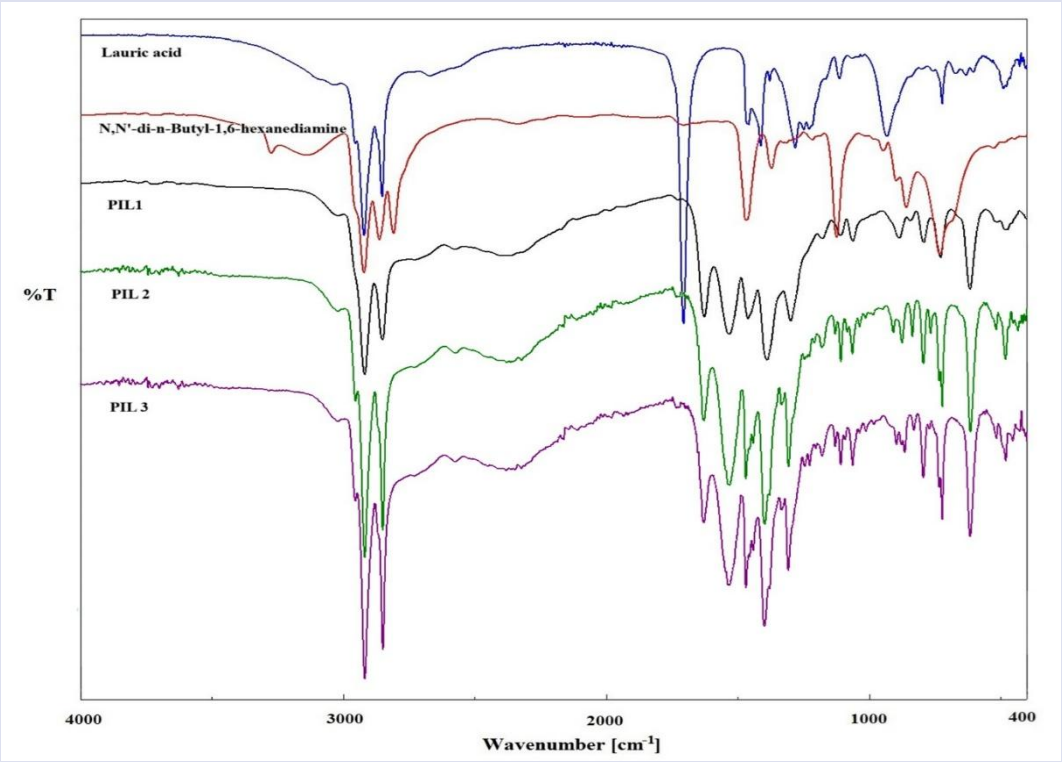

Figure 2. FT-IR spectra of precursors and PILs

Table 1. FT-IR spectrum data of PILs

ν, cm-1	PIL1	PIL2	PIL3
(NH2+)asy, sym	3026, 2362	3022, 2364	3022, 2381
Aliph. (C-H)asy, sym	2921, 2851	2919, 2851	2918, 2850
(COO-)asy, sym	1630, 1395	1629, 1397	1629, 1397
Aliph. (C-N-C)	1106	1107	1108

The chemical shifts, multiplicities, and coupling constants of the PILs are presented in Tables 2 and Table 3, respectively, and contribute to the detailed interpretation of the ^1H and ^{13}C NMR spectra. The numbering of proton and carbon atoms in the salt structures is shown in Tables 2 and 3. Additionally, the ^1H and ^{13}C NMR spectra of the corresponding PILs are provided in Figures S1–S8.

The structural characteristics of the PIL synthesized via protonation of *N,N'*-Dibutyl-1,6-hexanediamine were comprehensively investigated using ^1H NMR spectroscopy. The broad NH proton signal observed at 1.04 ppm in the free amine shifted downfield to approximately 9.00 ppm upon protonation (Table 2), strongly supporting successful proton transfer and the formation of the cationic species.

Table 2. ^{1}H NMR spectral data of the PILs. Chemical shifts (δ) reported in ppm and J values in Hz.

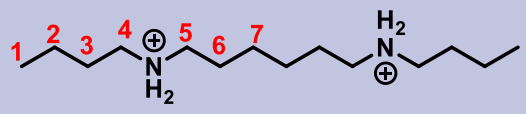

cationic moiety

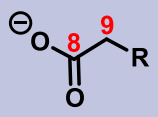

anionic moiety

C: 8-19; PIL1
C: 8-21; PIL2
C: 8-23; PIL3

	N,N'-Dibutyl-1,6-hexanediamine	PIL1	PIL2	PIL3
H1	0.82 (t, 6H, $^{3}J_{HH}$ 7.3)	0.86 (t, 6H, $^{3}J_{HH}$ 7.0)	0.84 (t, 6H, $^{3}J_{HH}$ 6.7)	0.86 (t, 6H, $^{3}J_{HH}$ 6.7)
H2,7	1.24 (m, 8H)	1.35 (m, 8H)	1.36 (m, 8H)	1.34 (m, 8H)
H3,6	1.37 (m, 8H)	1.64 (m, 8H)	1.63 (m, 8H)	1.64 (m, 8H)
H4,5	2.49 (t, 8H, $^{3}J_{HH}$ 7.2)	2.74 (q, 8H, $^{3}J_{HH}$ 6.2)	2.75 (q, 8H, $^{3}J_{HH}$ 7.1)	2.74 (q, 8H, $^{3}J_{HH}$ 6.5)
H9		2.13 (t, 4H, $^{3}J_{HH}$ 7.6)	2.14 (t, 4H, $^{3}J_{HH}$ 7.6)	2.14 (t, 4H, $^{3}J_{HH}$ 7.6)
H10		1.54 (m, 4H)	1.55 (m, 4H)	1.54 (m, 4H)
		1.23 (m, 32H) H11-H18	1.23 (m, 40H) H11-H20	1.23 (m, 48H) H11-H22
		0.89 (t, 6H, $^{3}J_{HH}$ 7.5) H19	0.90 (t, 6H, $^{3}J_{HH}$ 7.3) H21	0.90 (t, 6H, $^{3}J_{HH}$ 7.3) H23
NH	1.04 (sb, 2H)	-	-	-
$-NH_2^+$		8.91 (sb, 4H)	9.16 (sb, 4H)	9.09 (sb, 4H)

Characteristic proton resonances corresponding to the carboxylate anion clearly indicate the preservation of the anionic structure throughout the protonation process. Moreover, the significant downfield shift of the nitrogen-bond methylene protons (H4 and H5) from 2.49 to approximately 2.74 ppm reveals substantial decreases in electron density and notable changes in the local environment induced by protonation. Additionally, the absence of signals corresponding to the R-COOH protons of the fatty acids, typically observed around 11-12 ppm in ^{1}H NMR spectra, confirms the complete deprotonation of the carboxylic acid groups and successful conversion to the anionic form. These findings provide critical insights into the structural verification of both the cationic and anionic components of the PIL, thereby confirming the effectiveness of the synthetic approach.

Structural analysis of PILs via ^{13}C NMR spectroscopy has demonstrated that protonation predominantly occurs at the nitrogen center, leading to significant shifts in the chemical environments of carbon atoms directly bonded to nitrogen. The protonation process alters the electronic structure of the molecule, which is reflected in the ^{13}C NMR spectrum as general upfield (lower ppm) shifts. These findings confirm the successful protonation of the *N,N'*-Dibutyl-1,6-hexanediamine and, consequently, the formation of the targeted PIL. The spectral analysis also clearly revealed the structural integrity of the anionic moiety within the system. The signal observed around ~180 ppm (Table 3) corresponds to the carboxyl carbon, confirming the conversion of palmitic acid to its carboxylate form. Meanwhile, the characteristic cluster of signals around 14-38 ppm, attributed to the methylene groups in the aliphatic chain, indicates the chemically homogeneous nature of the hydrocarbon backbone. Terminal methyl and α-carbon atoms (C9), which are more susceptible to environmental influences, exhibited more distinct and separate signals. The obtained data strongly supports the preservation of structural integrity for both the cationic and anionic components after synthesis, affirming the successful formation of the intended PILs.

Table 3. ^{13}C NMR spectral data of the PILs. Chemical shifts (δ) reported in ppm.

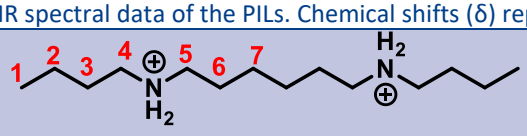

cationic moiety

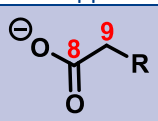

anionic moiety

C: 8-19; PIL1
C: 8-21; PIL2
C: 8-23; PIL3

	N,N'-Dibutyl-1,6-hexanediamine	PIL1	PIL2	PIL3
C1	13.99	13.84	13.85	13.85
C2	20.51	20.36	20.36	20.37
C3	32.34	29.00	28.95	29.04
C4	50.08	48.16	48.18	48.20
C5	49.81	48.03	48.04	48.08
C6	30.27	26.72	26.71	26.72
C7	27.37	26.64	26.63	26.69
C8		180.23	180.17	180.19
C9		38.04	38.00	38.03
C10		26.58	26.58	26.62
C11		29.48	29.49	29.49
		29.79 (C12-C13)	29.80 (C12)	29.79 (C12)
		29.81 (C14)	29.85 (C13-C17)	29.80 (C13)
		29.84 (C15)	29.92 (C18)	29.84 (C14-C19)
		29.92 (C16)	32.05 (C19)	29.93 (C20)
		32.04 (C17)	22.81 (C20)	32.05 (C21)
		22.80 (C18)	14.23 (C21)	22.81 (C22)
		14.21 (C19)		14.22 (C23)

Investigation of Thermal Behavior of PILs

DSC is the most widely used technique for evaluating the TES properties of PCMs, as it provides reliable data for assessing key parameters such as melting-solidification temperatures, enthalpies of phase transition, subcooling, total enthalpy, and specific heat capacity. The DSC thermograms of the synthesized PILs, along with the thermal data derived from the analysis, are illustrated in Figure 3 and Table 4. Furthermore, Table 4 presents the melting and freezing temperatures, as well as the thermal energy storage capacities, of the pure fatty acids utilized [43]. The melting temperatures of lauric, myristic, and palmitic acid were recorded at 315.29, 325.59, and 333.60 K, respectively, in agreement with the literature [44]. The solidification temperatures were measured 315.35, 325.64, and 333.03 K, respectively [44]. The energy storage capabilities of fatty acids were determined during both the melting and solidification processes. The melting enthalpies of lauric, myristic, and palmitic acids were 190.12 J/g (38.08 kJ/mol), 210.70 J/g (48.12 kJ/mol), and 221.42 J/g (56.78 kJ/mol), respectively, and the solidification enthalpies were 194.23 J/g (38.91 kJ/mol), 212.65 J/g (48.55 kJ/mol), and 226.56 J/g (58.09 kJ/mol), respectively, and are consistent with the values reported in the literature [45]. As the chain length of the molecule increased, so did the melting temperatures and energy storage capacities of fatty acids.

Upon examining the DSC analyses of PILs synthesized from *N,N'*-Dibutyl-1,6-hexanediamine and fatty acids, it was observed that there was an increase in the melting temperatures of the resulting PILs, accompanied by a slight decrease in their energy storage capacity. The melting temperature of the lauric acid-based PIL was found to be 354.26 K, whereas the solidification temperature was recorded at 335.06 K. The enthalpy of the same salt measured 110.85 J/g (69.73 kJ/mol), whereas the solidification enthalpy was recorded at 102.32 J/g (64.36 kJ/mol). The melting and solidification temperatures of the myristic acid-based PIL were determined to be 355.54 K and 338.64 K, respectively. The enthalpies of melting and solidification were quantified at 129.50 J/g (88.73 kJ/mol) and 112.33 J/g (76.96 kJ/mol), respectively. In palmitic acid-based PIL, the melting and solidification temperatures were calculated at 360.42 K and 348.54 K, while the energy storage capacities during the melting and solidification periods were quantified as 133.48 J/g (98.95 kJ/mol) and 129.63 J/g (96.09 kJ/mol), respectively. As the chain length increases in the synthesized PILs, the melting temperatures and melting enthalpies are also observed to increase. Furthermore, a notable rise in supercooling temperatures was recorded following the transition of energy storage materials from fatty acids to salts with varying chain lengths. The synthesized materials have potential as novel PCMs for energy storage applications due to their thermal durability and high energy storage capacity compared to PCMs based on ionic liquids [46,47].

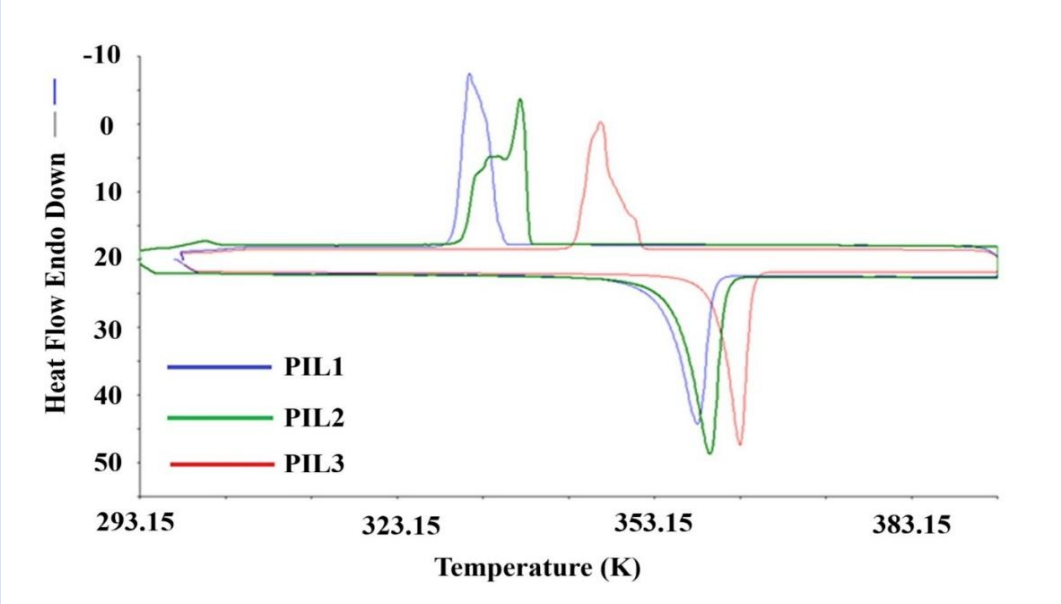

Figure 3. DSC curves of PILs

Table 4. Thermal data of fatty acids and PILs

Material	Melting Point (K)	Melting Enthalpy (J/g ; kJ/mol)	Freezing Point (K)	Freezing Enthalpy (J/g ; kJ/mol)
Lauric acid [43]	315.29	190.12; 38.08	315.35	194.23; 38.91
Myristic acid [43]	325.59	210.70; 48.12	325.64	212.65; 48.56
Palmitic acid [43]	333.60	221.42; 56,78	333.03	226.56; 58.09
PIL1	354.26	110.85; 69.73	335.06	102.32, 64.36
PIL2	355.54	129.50; 88.73	338.64	112.33; 76.96
PIL3	360.42	133.48; 98.95	348.54	126.63; 96.09

Thermal endurance of the PILs

TGA is essential for identifying the maximum operational temperature of PCMs by preventing chemical degradation. The onset temperature of degradation is a key parameter that defines the usable temperature range of PCMs. Figure 4 and Table 5 illustrate that three distinct chain lengths of PILs demonstrated a two-step degradation behavior. The initial decomposition phase of the lauric acid-based PIL commenced at 462.11 K and concluded at 575.69 K. The second decomposition phase commenced at 575.69 K and concluded at 694.78 K. In the initial phase, 59.57% of the material by mass underwent decomposition, while 29.04% by mass decomposed in the subsequent phase. The second salt derived from myristic acid demonstrated a two-step decomposition pattern, with 64.73% by mass decomposing between 468.54 and 593.69 K in the initial step, and 27.36% by mass decomposing between 593.69 and 720.56 K in the subsequent step. The third salt derived from palmitic acid exhibited thermal stability within the range of 473.63-612.98 K during the initial decomposition phase and 612.98-734.46 K during the subsequent decomposition phase. In the initial decomposition phase, 65.51% of the material was lost by mass, whereas 31.82% was lost in the subsequent decomposition phase. In PILs, thermal decomposition generally begins with the dissociation of the anion, followed by cationic decomposition [48]. In the synthesized PILs, the first degradation step belongs to the anionic part, while the second necking step indicates the cationic part. Long-chain anions more readily convert to volatile particles with increasing temperature, while mass loss in TG increases and the amount of residue decreases. In all PILs, the source of the remaining mass without decomposition above 773.15 K is carbon. Thermal analysis data of PIL1, PIL2, and PIL3 reveal that an increase in molecular weight corresponds to enhanced thermal resistance, as observed from PIL1 to PIL3. The generated materials exhibit thermal resistance suitable for application in elevated temperature environments.

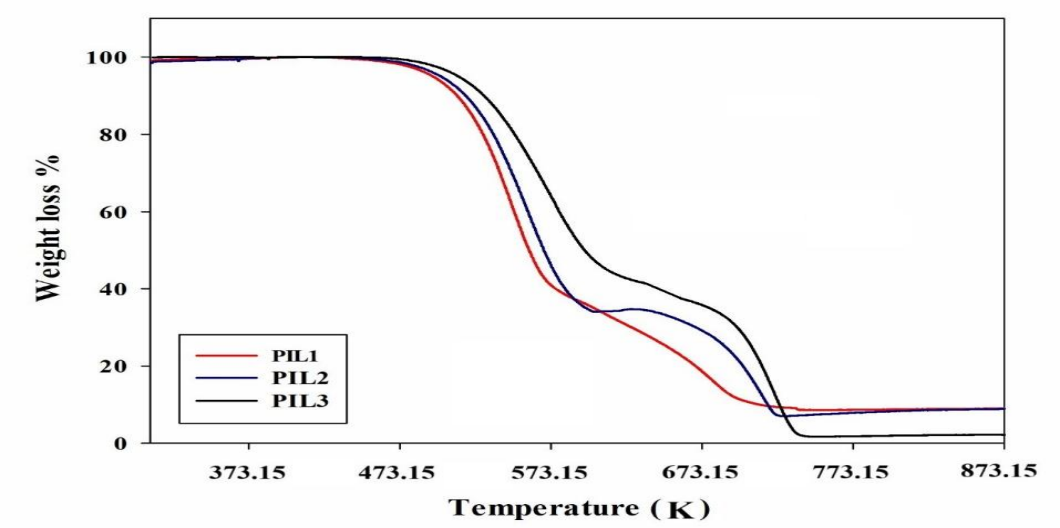

Figure 4. TGA curves of PILs

Table 5. TGA data of PILs

Material	First degradation temperature (K)	Weight loss [%]	Second degradation temperature (K)	Weight loss [%]
PIL1	462.11-575.69	59.57	575.69 -694.78	29.04
PIL2	468.54-593.69	64.73	593.69-720.56	27.36
PIL3	473.63-612.98	65.51	612.98-734.46	31.82

Thermal reliability of the PILs

PCMs selected as thermal energy storage materials are expected to be structurally and thermally stable after repeated heating-cooling cycles. The structural stability and thermal reliability of the synthesized PILs were investigated by repeating FT-IR and DSC analyses after 1000 melting and freezing cycles. The FT-IR spectra of PCMs were shown in Figure 5 before and after heat cycling, in comparison. The forms and locations of peaks do not alter following thermal cycling. By analyzing the chemical structure of the produced PCMs after 1000 heat cycles, FT-IR data showed that there is no deterioration, decomposition, or sublimation.

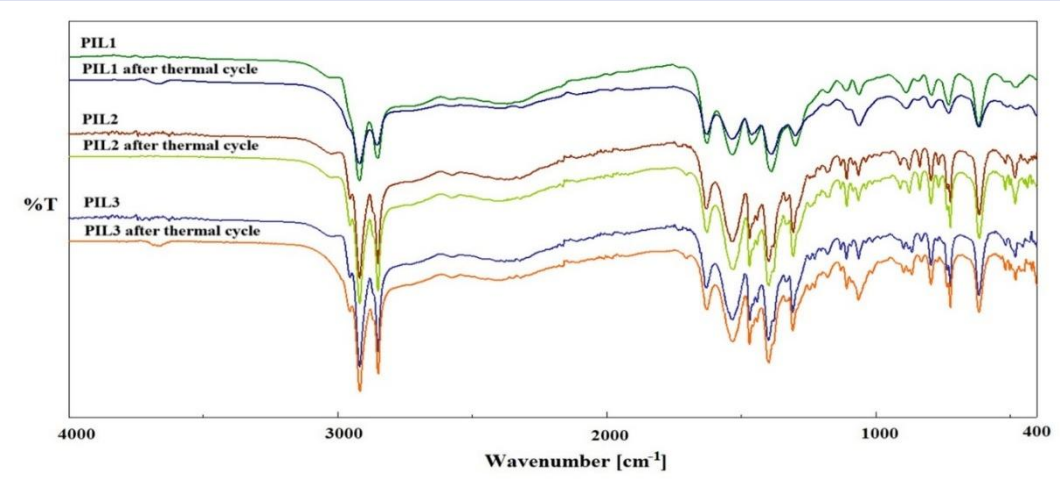

Figure 5. FT-IR spectra PILs before and after thermal cycling

Moreover, Figure 6 illustrates the DSC curves of the PILs prior to and following 1000 thermal cycles, while Table 6 presents the corresponding DSC data for these salts before and after the thermal cycling process. The DSC results indicate that there was no notable alteration in the melting and solidification temperatures of the synthesized protic molten salts throughout 1000 successive thermal cycles. Conversely, the phase change enthalpies of phase change materials exhibited a slight reduction in comparison to their uncycled counterparts. The alterations in melting enthalpy were minimal, recorded at 2.67%, 0.05%, and 0.232% for PIL1, PIL2, and PIL3, respectively. Thermal cycling chemically or physically disrupts the structure of PCM, reducing the amount of latent heat (enthalpy) stored or released during the phase change. This leads to a decrease in the material's heat storage capacity and melting temperature over time [49,50]. Nonetheless, this reduction is not significant enough to impact the functionality of the material in energy storage applications.

Table 6. Thermal behavior of fatty acids and PILs pre- and post-thermal cycling

Material	Melting Point (K)	Melting Enthalpy (J/g ; kJ/mol)	Freezing Point (K)	Freezing Enthalpy (J/g ; kJ/mol)
PIL1	354.26	110.85; 69.73	335.06	102.32, 64.36
PIL1 after thermal cycling	354.82	107.89; 67.87	335.15	95.45 60.04
PIL2	355.54	129.50; 88.73	338.64	112.33; 76.96
PIL2 after thermal cycling	355.49	129.43; 88.68	340.82	115.88; 79.40
PIL3	360.42	133.48; 98.95	348.54	126.63; 96.09
PIL3 after thermal cycling	360.14	133.17; 98.71	346.49	125.05; 92.70

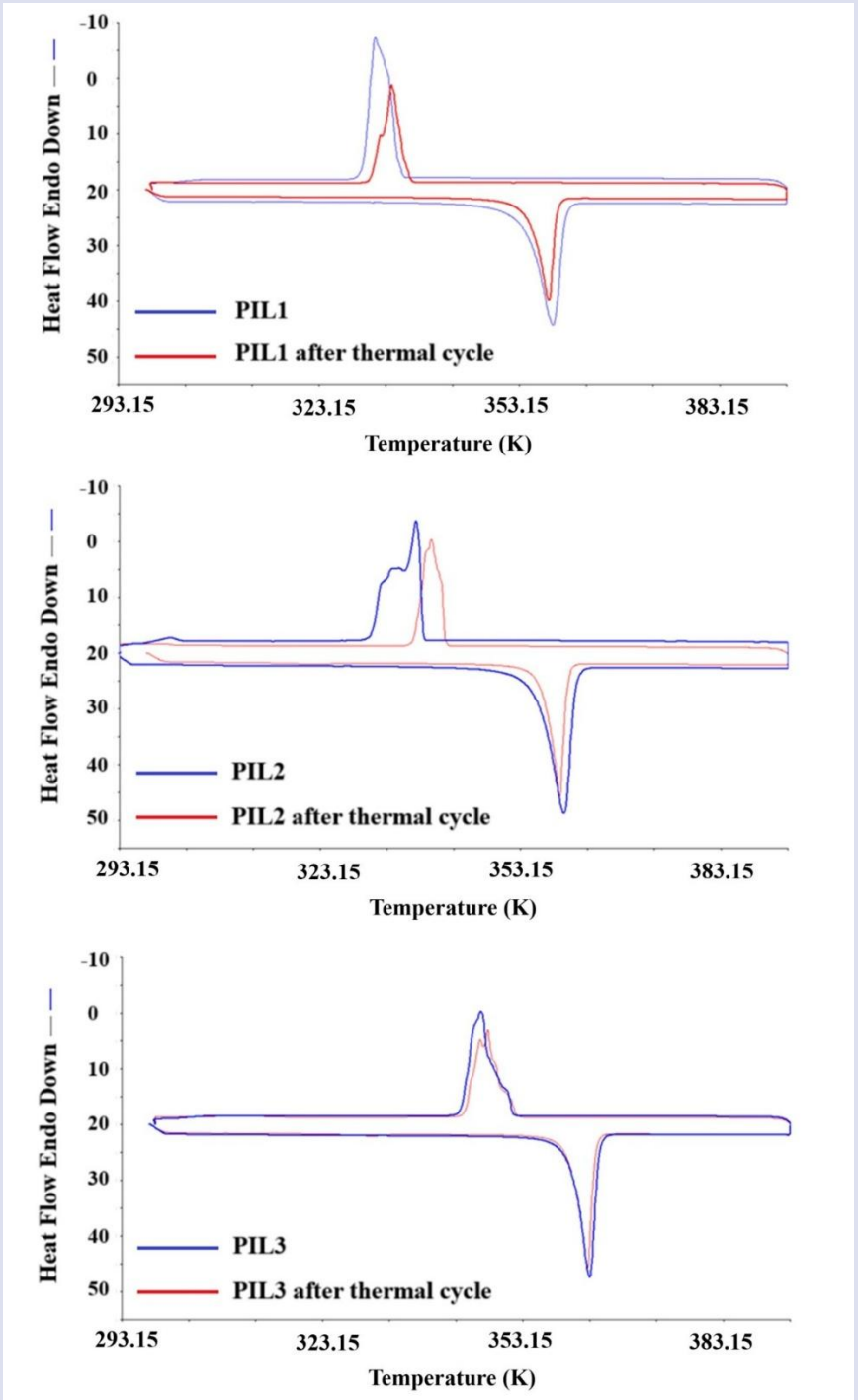

Figure 6. DSC curves of PILs pre- and post-thermal cycling

Conclusion

In this study, PILs derived from N,N'-Dibutyl-1,6-hexanediamine and various fatty acids (lauric, palmitic, and myristic acids) were successfully synthesized and structurally characterized. FT-IR analysis confirmed the formation of ionic bonds indicative of effective proton transfer, while ^{1}H and ^{13}C NMR spectroscopy provided detailed insights into molecular structure and environmental changes upon protonation. The spectral data demonstrated that the ILs maintain structural integrity with clear evidence of protonation at the amine sites and deprotonation of the carboxylic acids. The melting points of the phase change materials were documented within the range of 354.26 to 360.42 K, as determined by DSC analyses. The latent heat of fusion was found to be 69.73, 88.73, and 98.95 kJ/mol for PIL1, PIL2, and PIL3, respectively. The TGA results indicated that the synthesized PILs demonstrated a two-step decomposition behavior and maintained thermal stability up to approximately 463.15 K. The findings from both DSC and TGA analyses indicated that an increase in the chain length of the PILs corresponded with enhanced latent heat storage capacity and improved thermal stability. Following 1000 consecutive thermal cycles at temperatures ranging from 293.15 to 393.15 K, the produced PILs underwent structural and thermal testing once more. The structural stability of the PILs was confirmed, while the phase change enthalpies of the PCMs exhibited a minor reduction in comparison to their non-cyclic counterparts. These findings establish a comprehensive understanding of the molecular interactions within the synthesized PILs, supporting their potential applicability in areas such as thermal energy storage and green solvents. Future studies focusing on the physicochemical properties and application performance of these materials are warranted to further explore their practical utility.

Conflicts of interest

There are no conflicts of interest in this work.

References

[1] Martins F., Felgueiras C., Smitkova M., Caetano N., Analysis of Fossil Fuel Energy Consumption and Environmental Impacts in European Countries, *Energies*, 12 (2019) 964.

[2] Dincer I., Thermal energy storage systems as a key technology in energy conservation, *Int. J. Energy Res.*, 26 (2002) 567–588.

[3] Nazir H., Batool M., Bolivar Osorio F.J., Isaza-Ruiz M., Xu X., Vignarooban K., et al., Recent developments in phase change materials for energy storage applications: A review, *Int. J. Heat Mass Transf.*, 129 (2019) 491–523.

[4] Ismail M.M., Dincer I., Bicer Y., Saghir M.Z., Nanoparticles enhanced phase change materials for thermal energy storage applications: An assessment, *Int. J. Thermofluids*, 27 (2025) 101207.

[5] Powell K.M., Kim J.S., Cole W.J., Kapoor K., Mojica J.L., Hedengren J.D., et al., Thermal energy storage to minimize cost and improve efficiency of a polygeneration district energy system in a real-time electricity market, *Energy*, 113 (2016) 52–63.

[6] Sarbu I., Sebarchievici C., A Comprehensive Review of Thermal Energy Storage, *Sustainability*, 10 (2018) 191.

[7] Hussain A., Arif S.M., Aslam M., Emerging renewable and sustainable energy technologies: State of the art, *Renew. Sustain. Energy Rev.*, 71 (2017) 12–28.

[8] Farid M., Khudhair A.M., Razack S.A.K., Al-Hallaj S., A Review on Phase Change Energy Storage: Materials and Applications, in: *Thermal Energy Storage with Phase Change Materials*, (2021) 4–23.

[9] Ismail K.A.R., Lino F.A.M., Machado P.L.O., Teggar M., Arıcı M., Alves T.A., et al., New potential applications of phase change materials: A review, *J. Energy Storage*, 53 (2022) 105202.

[10] Javadi F.S., Metselaar H.S.C., Ganesan P., Performance improvement of solar thermal systems integrated with phase change materials (PCM), a review, *Sol. Energy*, 206 (2020) 330–352.

[11] Lin Y., Jia Y., Alva G., Fang G., Review on thermal conductivity enhancement, thermal properties and applications of phase change materials in thermal energy storage, *Renew. Sustain. Energy Rev.*, 82 (2018) 2730–2742.

[12] Mohamed S.A., Al-Sulaiman F.A., Ibrahim N.I., Zahir M.H., Al-Ahmed A., Saidur R., et al., A review on current status and challenges of inorganic phase change materials for thermal energy storage systems, *Renew. Sustain. Energy Rev.*, 70 (2017) 1072–1089.

[13] Magendran S.S., Khan F.S.A., Mubarak N.M., Vaka M., Walvekar R., Khalid M., et al., Synthesis of organic phase change materials (PCM) for energy storage applications: A review, *Nano-Struct. Nano-Objects*, 20 (2019) 100399.

[14] Dincer I., Evaluation and selection of energy storage systems for solar thermal applications, *Int. J. Energy Res.*, 23 (1999) 1017–1028. https://doi.org/10.1002/(SICI)1099-114X(19991010)23:12<1017::AID-ER535>3.0.CO;2-Q.

[15] Soares N., Costa J.J., Gaspar A.R., Santos P., Review of passive PCM latent heat thermal energy storage systems towards buildings' energy efficiency, *Energy Build.*, 59 (2013) 82–103.

[16] Baetens R., Jelle B.P., Gustavsen A., Phase change materials for building applications: A state-of-the-art review, *Energy Build.*, 42 (2010) 1361–1368.

[17] Milián Y.E., Gutiérrez A., Grágeda M., Ushak S., A review on encapsulation techniques for inorganic phase change materials and the influence on their thermophysical properties, *Renew. Sustain. Energy Rev.*, 73 (2017) 983–999.

[18] Wang X., Zhang Y., Xiao W., Zeng R., Zhang Q., Di H., Review on thermal performance of phase change energy storage building envelope, *Chin. Sci. Bull.*, 54 (2009) 920–928.

[19] Cabeza L.F., Castell A., Barreneche C., de Gracia A., Fernández A.I., Materials used as PCM in thermal energy storage in buildings: A review, *Renew. Sustain. Energy Rev.*, 15 (2011) 1675–1695.

[20] Zalba B., Marín J.M., Cabeza L.F., Mehling H., Review on thermal energy storage with phase change: materials, heat transfer analysis and applications, *Appl. Therm. Eng.*, 23 (2003) 251–283.

[21] Sharma A., Tyagi V.V., Chen C.R., Buddhi D., Review on thermal energy storage with phase change materials and applications, *Renew. Sustain. Energy Rev.*, 13 (2009) 318–345.

[22] Farid M.M., Khudhair A.M., Razack S.A.K., Al-Hallaj S., A review on phase change energy storage: materials and applications, *Energy Convers. Manag.*, 45 (2004) 1597–1615.

[23] Liu M., Saman W., Bruno F., Review on storage materials and thermal performance enhancement techniques for high temperature phase change thermal storage systems, *Renew. Sustain. Energy Rev.*, 16 (2012) 2118–2132.

[24] Guo X., Study on inorganic PCMs modification utilized in building environment for energy conservation, *Energy Sources Part A*, (2024).

[25] Liu L., Li J., Deng Y., Yang Z., Huang K., Zhao S., Optimal design of multi-layer structure composite containing inorganic hydrated salt phase change materials and cement: Lab-scale tests for buildings, *Constr. Build. Mater.*, 275 (2021) 122125.

[26] Cui H., Zhang W., Yang H., Zou Y., Liu J., Yan J., Preparation and investigation of a prefabricated salt hydrate phase change material partition for passive solar buildings, *Energy*, 303 (2024) 132010.

[27] Nartowska E., Styś-Maniara M., Kozłowski T., The potential environmental and social influence of the inorganic salt hydrates used as a phase change material for thermal energy storage in solar installations, *Int. J. Environ. Res. Public Health*, 20 (2023) 1331.

[28] Wang Q., Wu C., Wang X., Sun S., Cui D., Pan S., et al., A review of eutectic salts as phase change energy storage materials in the context of concentrated solar power, *Int. J. Heat Mass Transf.*, 205 (2023) 123904.

[29] Galazutdinova Y., Al-Hallaj S., Grágeda M., Ushak S., Development of the inorganic composite phase change materials for passive thermal management of Li-ion batteries: material characterization, *Int. J. Energy Res.*, 44 (2020) 2011–2022.

[30] Dai X., Ping P., Kong D., Luo X., Wang G., Ren J., et al., Experimental investigation on flexible inorganic phase change material for thermal management performance improvement of lithium-ion battery, *Appl. Therm. Eng.*, 272 (2025) 126358.

[31] Galazutdinova Y., Ushak S., Farid M., Al-Hallaj S., Grágeda M., Development of the inorganic composite phase change materials for passive thermal management of Li-ion batteries: Application, *J. Power Sources*, 491 (2021) 229624.

[32] Ping P., Dai X., Kong D., Zhang Y., Zhao H., Gao X., et al., Experimental study on nano-encapsulated inorganic phase change material for lithium-ion battery thermal management and thermal runaway suppression, *Chem. Eng. J.*, 463 (2023) 142401.

[33] Ushak S., Gutierrez A., Barreneche C., Fernandez A.I., Grágeda M., Cabeza L.F., Reduction of the subcooling of bischofite with the use of nucleating agents, *Sol. Energy Mater. Sol. Cells*, 157 (2016) 1011–1018.

[34] Dannemand M., Johansen J.B., Furbo S., Solidification behavior and thermal conductivity of bulk sodium acetate trihydrate composites with thickening agents and graphite, *Sol. Energy Mater. Sol. Cells*, 145 (2016) 287–295.

[35] Sun W., Zhang Y., Ling Z., Fang X., Zhang Z., Experimental investigation on the thermal performance of double-layer PCM radiant floor system containing two types of inorganic composite PCMs, *Energy Build.*, 211 (2020) 109806.

[36] Zhang Y., Liu S., Yang L., Yang X., Shen Y., Han X., Experimental Study on the Strengthen Heat Transfer Performance of PCM by Active Stirring, *Energies*, 13 (2020) 2238.

[37] Mokhtarpour M., Rostami A., Shekaari H., Zarghami A., Faraji S., Novel protic ionic liquids-based phase change materials for high performance thermal energy storage systems, *Sci. Rep.*, 13 (2023) 1–10.

[38] Mokhtarpour M., Rostami A., Shekaari H., Zarghami A., Faraji S., Thermal properties of novel phase change materials based on protic ionic liquids containing ethanolamines and stearic acid for efficient thermal energy storage, *Phys. Chem. Chem. Phys.*, 26 (2024) 13839–13849.

[39] Mokhtarpour M., Rostami A., Shekaari H., Zarghami A., Faraji S., Protic ionic liquids mono, di, triethanolamine laurate as green phase change materials: thermal energy storage capacity and conversion to electricity, *J. Therm. Anal. Calorim.*, 149 (2024) 7169–7177. https://doi.org/10.1007/s10973-024-13270-w.

[40] Lopez-Morales J.L., Perez-Arce J., Serrano A., Dauvergne J.L., Casado N., Kottarathil A., et al., Protic dialkylammonium-based ionic liquids as promising solid-solid phase change materials for thermal energy storage: Synthesis and thermo-physical characterization, *J. Energy Storage*, 72 (2023) 108379.

[41] Faraji S., Shekaari H., Zafarani-Moattar M.T., Mokhtarpour M., Experimental studies on thermophysical properties of protic ionic liquids for thermal energy storage systems, *J. Energy Storage*, 54 (2022) 105251.

[42] Kaljusmaa L.M., Tubli D., Adamson J., Konist A., Järvik O., Thermal stability of amine and carboxylic acid based protic ionic liquids from the perspective of thermal energy storage, *J. Mol. Liq.*, 427 (2025) 127396.

[43] Alkan C., Sari A., Fatty acid/poly(methyl methacrylate) (PMMA) blends as form-stable phase change materials for latent heat thermal energy storage, *Sol. Energy*, 82 (2008) 118–124.

[44] Lin C., Li W., Yan Y., Ke H., Liu Z., Deng L., et al., Ultrafine electrospun fiber based on ionic liquid/AlN/copolyamide composite as novel form-stable phase change material for thermal energy storage, *Sol. Energy Mater. Sol. Cells*, 223 (2021) 110953.

[45] Zhu J., Bai L., Chen B., Fei W., Thermodynamical properties of phase change materials based on ionic liquids, *Chem. Eng. J.*, 147 (2009) 58–62.

[46] Xu C., Cheng Z., Thermal Stability of Ionic Liquids: Current Status and Prospects for Future Development, *Processes*, 9 (2021) 337.

[47] Sarı A., Biçer A., Lafçı Ö., Ceylan M., Galactitol hexa stearate and galactitol hexa palmitate as novel solid–liquid phase change materials for thermal energy storage, *Sol. Energy*, 85 (2011) 2061–2071.